arXiv:1612.06116v2 [hep-ex] 21 Dec 2016

EUROPEAN ORGANIZATION FOR NUCLEAR RESEARCH (CERN)

CERN-EP-2016-298
LHCb-PAPER-2016-051
December 19, 2016

Measurement of the ratio of branching fractions and difference in *CP* asymmetries of the decays $B^+ \to J/\psi\,\pi^+$ and $B^+ \to J/\psi\,K^+$

The LHCb collaboration[†]

Abstract

The ratio of branching fractions and the difference in *CP* asymmetries of the decays $B^+ \to J/\psi\,\pi^+$ and $B^+ \to J/\psi\,K^+$ are measured using a data sample of pp collisions collected by the LHCb experiment, corresponding to an integrated luminosity of $3\,\text{fb}^{-1}$ at centre-of-mass energies of 7 and 8 TeV. The results are

$$\frac{\mathcal{B}(B^+ \to J/\psi\,\pi^+)}{\mathcal{B}(B^+ \to J/\psi\,K^+)} = (3.83 \pm 0.03 \pm 0.03) \times 10^{-2}\,,$$

$$\mathcal{A}^{CP}(B^+ \to J/\psi\,\pi^+) - \mathcal{A}^{CP}(B^+ \to J/\psi\,K^+) = (1.82 \pm 0.86 \pm 0.14) \times 10^{-2},$$

where the first uncertainties are statistical and the second are systematic. Combining this result with a recent LHCb measurement of $\mathcal{A}^{CP}(B^+ \to J/\psi\,K^+)$ provides the most precise estimate to date of *CP* violation in the decay $B^+ \to J/\psi\,\pi^+$,

$$\mathcal{A}^{CP}(B^+ \to J/\psi\,\pi^+) = (1.91 \pm 0.89 \pm 0.16) \times 10^{-2}.$$

Submitted to JHEP.

© CERN on behalf of the LHCb collaboration, licence CC-BY-4.0.

[†]Authors are listed at the end of this paper.

1 Introduction

In the Standard Model, the decay $B^+ \to J/\psi K^+$ proceeds via a $b \to c\bar{c}s$ quark transition[1] and, since this process is dominated by a Cabibbo-favoured tree diagram, it is expected to exhibit negligible *CP* violation [1]. By contrast, for the decay $B^+ \to J/\psi \pi^+$, which proceeds via $b \to c\bar{c}d$, *CP* violation up to the percent level can be generated by interference between the suppressed tree-level diagram and additional gluonic penguin (loop) diagrams as shown in Fig. 1. Measurements of the branching fraction and *CP* asymmetry of the decay $B^+ \to J/\psi \pi^+$ can provide information about the size of the penguin-diagram contributions relative to that of the tree diagram. This is critical for estimating the effects of penguin-diagram contributions in $b \to c\bar{c}s$ decays on the determination of the *CP* violation parameter $\sin 2\beta$ [2, 3].

The world average of the branching fraction $\mathcal{B}(B^+ \to J/\psi \pi^+)$ is $(4.1 \pm 0.4) \times 10^{-4}$ [4], with no significant *CP* asymmetry observed so far. The world average value of $\mathcal{A}^{CP}$ $(B^+ \to J/\psi \pi^+)$, which includes measurements from Belle, BaBar, D0 and LHCb [5–8], is $(1.0 \pm 2.8) \times 10^{-2}$ [4].

In an earlier analysis of a sample of *pp* collision data corresponding to an integrated luminosity of $0.37\,\text{fb}^{-1}$ [8], LHCb measured the *CP* asymmetry $\mathcal{A}^{CP}(B^+ \to J/\psi \pi^+) = (0.5 \pm 2.7 \pm 1.1) \times 10^{-2}$, as well as the ratio of branching fractions

$$\mathcal{R}_{\pi/K} \equiv \frac{\mathcal{B}(B^+ \to J/\psi \pi^+)}{\mathcal{B}(B^+ \to J/\psi K^+)} = (3.83 \pm 0.11 \pm 0.07) \times 10^{-2}. \quad (1)$$

This paper reports an update of the analysis and uses the full *pp* data sample from the LHC Run 1, corresponding to $1\,\text{fb}^{-1}$ collected at a centre-of-mass energy of 7 TeV and $2\,\text{fb}^{-1}$ at 8 TeV, and measures $\mathcal{R}_{\pi/K}$ and $\Delta\mathcal{A}^{CP} \equiv \mathcal{A}^{CP}(B^+ \to J/\psi \pi^+) - \mathcal{A}^{CP}(B^+ \to J/\psi K^+)$, where these two decays are reconstructed using the dimuon decay mode of the J/ψ meson. The result for $\Delta\mathcal{A}^{CP}$ is combined with the $\mathcal{A}^{CP}(B^+ \to J/\psi K^+)$ measurement from another LHCb analysis [9] to obtain $\mathcal{A}^{CP}(B^+ \to J/\psi \pi^+)$.

2 Detector and simulation

The LHCb detector [10, 11] is a single-arm forward spectrometer covering the pseudorapidity range $2 < \eta < 5$, designed for the study of particles containing b or c quarks. The detector includes a high-precision tracking system consisting of a silicon-strip vertex detector surrounding the *pp* interaction region, a large-area silicon-strip detector located upstream of a dipole magnet with a bending power of about 4 Tm, and three stations of silicon-strip detectors and straw drift tubes placed downstream of the magnet. The tracking system provides a measurement of momentum, p, of charged particles with a relative uncertainty that varies from 0.5% at low momentum to 1.0% at 200 GeV/c. The minimum distance of a track to a primary vertex (PV), the impact parameter, is measured with a resolution of $(15 + 29/p_{\text{T}})\,\mu\text{m}$, where p_{T} is the component of the momentum transverse to the beam, in GeV/c. Different types of charged hadrons are distinguished using information from two ring-imaging Cherenkov detectors. Photons, electrons and hadrons are identified by a calorimeter system consisting of scintillating-pad

[1] Unless otherwise specified, the inclusion of charge-conjugate processes is implied throughout this paper.

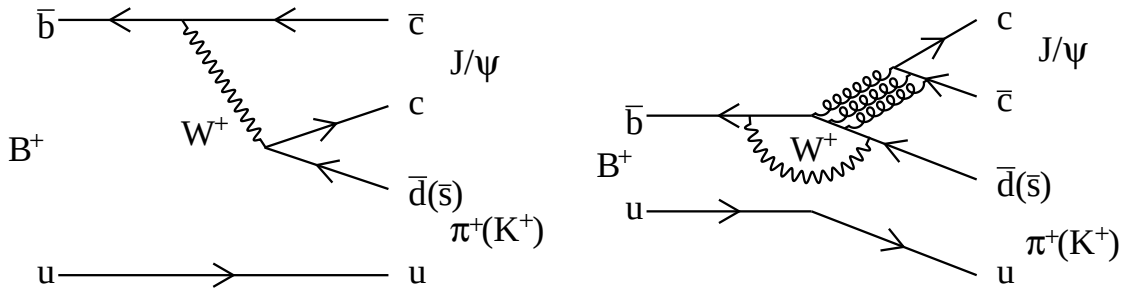

Figure 1: Feynman diagrams for $B^+ \to J/\psi\,\pi^+(K^+)$ decays at the tree (left) and one-loop (right) levels.

and preshower detectors, an electromagnetic calorimeter and a hadronic calorimeter. Muons are identified by a system composed of alternating layers of iron and multiwire proportional chambers. The online event selection is performed by a trigger [12], which consists of a hardware stage, based on information from the calorimeter and muon systems, followed by a software stage, which applies a full event reconstruction.

In this analysis, the hardware trigger decision is required to be caused by at least one high-$p_{\rm T}$ track that is consistent with being a muon. In the software trigger, two well-reconstructed muons with opposite charge are required to form a good-quality vertex and to have an invariant mass consistent with that of the J/ψ meson [4]. The trigger also requires a significant displacement between the J/ψ vertex and the associated PV of the pp collision.

In the simulation, pp collisions are generated using Pythia [13, 14] with a specific LHCb configuration [15]. Decays of hadronic particles are described by EvtGen [16], in which final-state radiation is generated using Photos [17]. The interaction of the generated particles with the detector, and its response, are implemented using the Geant4 toolkit [18] as described in Ref. [19].

3 Event selection

The same criteria are used to select $B^+ \to J/\psi\,\pi^+$ and $B^+ \to J/\psi\,K^+$ decays, except for those related to the identification of the final-state hadrons, and consist of a loose preselection followed by a multivariate selection. In the preselection, all three final-state tracks are required to be of good quality and within a fiducial region of the detector acceptance that excludes areas with large asymmetries in the detection efficiencies.

The J/ψ candidates are formed from two oppositely charged particles with $p_{\rm T}$ greater than $550\,{\rm MeV}/c$, identified as muons and consistent with originating from a common vertex but inconsistent with originating from any PV. The invariant mass of the $\mu^+\mu^-$ pair is required to be within $^{+43}_{-48}\,{\rm MeV}/c^2$ of the known J/ψ mass [4], then constrained to that value in subsequent stages of the reconstruction. The B^+ candidates are formed by combining each J/ψ candidate with a hadron candidate that has $p_{\rm T}$ greater than $1\,{\rm GeV}/c$ and p greater than $5\,{\rm GeV}/c$ and forms a common vertex with the J/ψ. Both the kaon and pion mass hypotheses of the hadron candidates are kept. Each reconstructed B^+ candidate is required to be consistent with originating from a PV. The vector from the

corresponding PV to the decay vertex of the B^+ is required to be closely aligned with the momentum vector of the B^+ candidate: the opening angle ϕ between them must satisfy $\cos\phi > 0.999$. To ensure a clean separation between the $B^+ \to J/\psi\pi^+$ and $B^+ \to J/\psi K^+$ mass peaks in the $J/\psi\pi^+$ mass spectrum, the decay angle θ_h, defined as the angle between the momentum of the kaon or pion in the B^+ rest frame and the B^+ momentum in the laboratory frame, is required to satisfy $\cos\theta_h < 0$ [8].

The $B^+ \to J/\psi\pi^+$ and $B^+ \to J/\psi K^+$ candidates passing the preselection are filtered using the output of a boosted decision tree (BDT) [20,21] to further suppress combinatorial background. The BDT uses kinematic and topological variables to discriminate between signal and background. These include the impact parameters of the final-state tracks with respect to the PV, as well as those of the J/ψ and the B^+ candidates, the $p_{\rm T}$ of the final-state hadron and the J/ψ and B^+ candidates, and the decay-length and vertex-fit χ^2 of the B^+ candidate. Given the similarity of their kinematic distributions, the same BDT classifier is used to select both decays. The BDT is trained using a simulated sample of $B^+ \to J/\psi\pi^+$ decays and a background sample consisting of candidates from the data sample passing the $B^+ \to J/\psi\pi^+$ preselection with invariant mass in the range 5500–5700 MeV/c^2.

Particle identification (PID) criteria are applied to select pion and kaon candidates, with the two hypotheses being mutually exclusive. The requirements on the BDT response and PID are chosen to maximise the figure of merit for the decay $B^+ \to J/\psi\pi^+$, defined as $N_\pi/\sqrt{N_{\rm tot}}$, where $N_{\rm tot}$ is the total number of $B^+ \to J/\psi\pi^+$ candidates within ± 3 times the mass resolution around the known B^+ mass. Here N_π refers to the $B^+ \to J/\psi\pi^+$ signal yield and is estimated to be $(N_{\rm tot} - N_{\rm comb})/(1 + 1/(r_{\rm eff}\mathcal{R}_{\pi/K}))$, where the value of $\mathcal{R}_{\pi/K}$ is given in Eq. 1, $N_{\rm comb}$ is the number of combinatorial background events in the $B^+ \to J/\psi\pi^+$ signal region extrapolated from the region 5340–5580 MeV/c^2 passing the PID selection, and $r_{\rm eff}$ is the ratio of the efficiencies for $B^+ \to J/\psi\pi^+$ and $B^+ \to J/\psi K^+$ events to pass the $B^+ \to J/\psi\pi^+$ selection and fall in the signal window, estimated from simulation. After this optimisation, the BDT rejects more than 85% of the combinatorial background and retains around 92% of $B^+ \to J/\psi h^+$ events, where $h = \pi, K$. The particle identification requirement has an efficiency of about 97% for $B^+ \to J/\psi\pi^+$ and 69% for $B^+ \to J/\psi K^+$. The fraction of events in which more than one candidate passes the selection is negligible.

4 Signal yield determination

The signal yields $N_{J/\psi h}$ and raw charge asymmetries $A^{\rm raw}_{J/\psi h}$ of the two decay modes are determined from independent unbinned extended maximum likelihood fits to the invariant mass distributions of $B^+ \to J/\psi h^+$ and $B^- \to J/\psi h^-$. Denoting the signal yield for $B^\pm \to J/\psi h^\pm$ by $N_{J/\psi h^\pm}$, $N_{J/\psi h}$ is the sum of $B^- \to J/\psi\pi^-$ and $B^+ \to J/\psi\pi^+$, and $A^{\rm raw}_{J/\psi h}$ is defined as

$$A^{\rm raw}_{J/\psi h} = \frac{N_{J/\psi h^-} - N_{J/\psi h^+}}{N_{J/\psi h^-} + N_{J/\psi h^+}}. \tag{2}$$

The fits use $B^+ \to J/\psi\pi^+$ candidates in the range 5000–5600 MeV/c^2 and $B^+ \to J/\psi K^+$ candidates in the range 5000–5700 MeV/c^2. The B^+ and B^- samples are fitted simultaneously, as shown in Figs. 2 and 3. Table 1 summarizes the fit results for the parameters

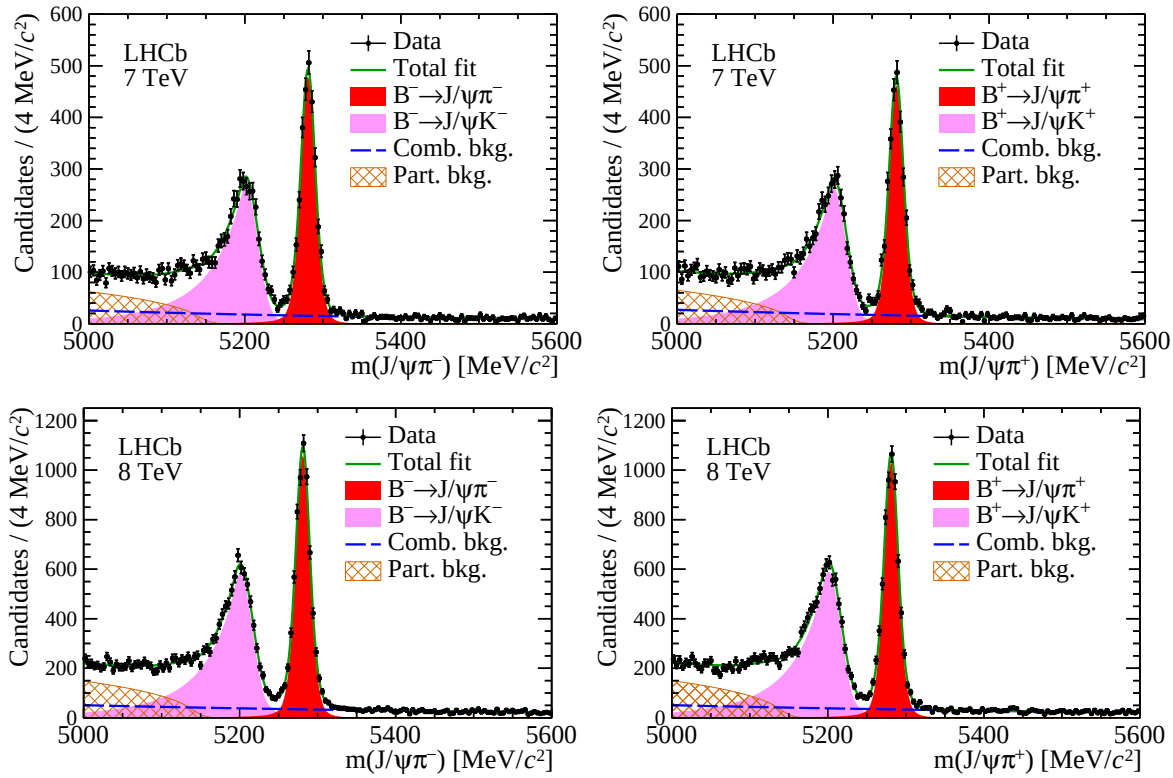

Figure 2: Invariant mass distributions of (left) $B^- \to J/\psi\pi^-$ and (right) $B^+ \to J/\psi\pi^+$ candidates with the result of the fit superimposed, for data collected at (top) 7 TeV and (bottom) 8 TeV.

of interest. In each fit, the signal shape is modelled by a Hypatia function [22]. The most probable value and the resolution of the Hypatia function are allowed to vary in the fit, while the tail parameters are fixed to values determined from fits to simulated events. The hadron misidentification background in the $B^+ \to J/\psi\pi^+$ sample, arising from $B^+ \to J/\psi K^+$ decays in which the kaon is misidentified as a pion, is described by a double-sided Crystal Ball (DSCB) function whose parameters, except for the most probable value and the core width, are fixed to values determined from fits to simulated events. The misidentification background due to $B^+ \to J/\psi\pi^+$ decays in which the pion is misidentified as a kaon is neglected in the baseline fit; a systematic uncertainty due to this assumption is assigned, as discussed in Sec. 6. The combinatorial background is modelled by an exponential function whose shape parameter is left free in the fit. The background due to partially reconstructed B-meson decays such as $B \to J/\psi h\pi$ is described by an ARGUS function [23] convolved with a Gaussian function, with all parameters allowed to vary in the fit. Contributions from the highly suppressed $B^+ \to K^+\mu^+\mu^-$ [4] and $B^+ \to \pi^+\mu^+\mu^-$ [24] decays are negligible.

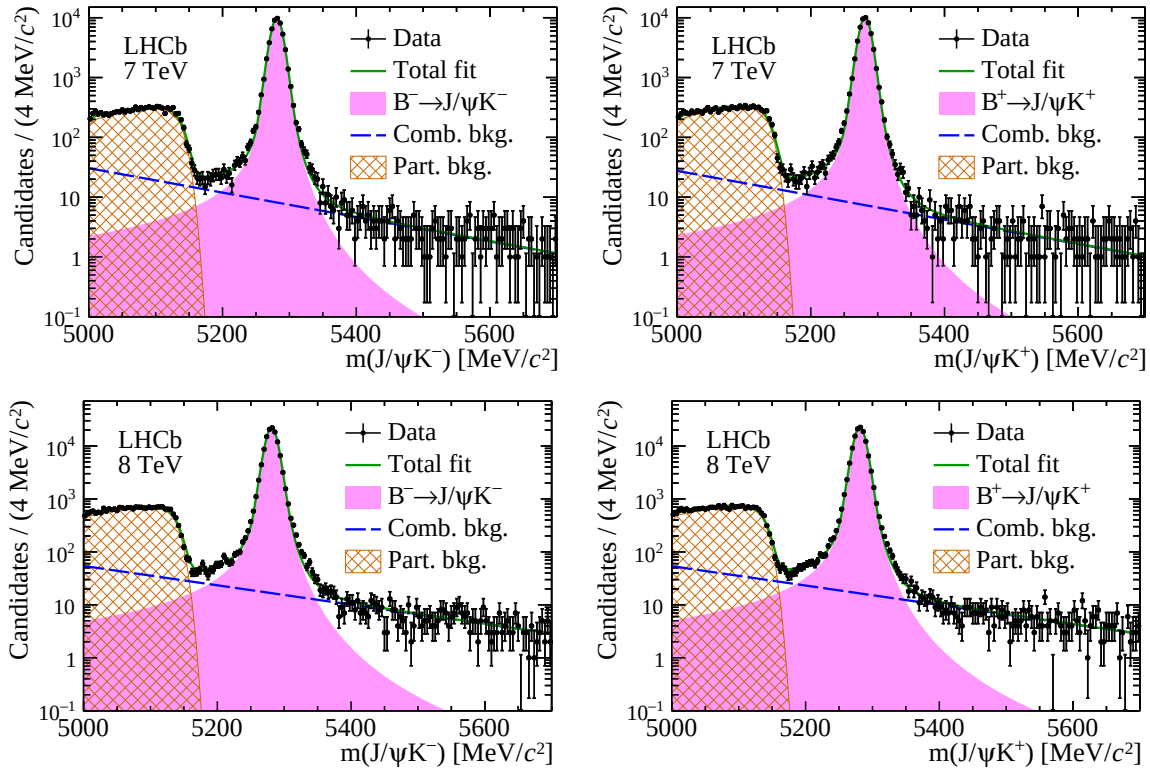

Figure 3: Invariant mass distributions of (left) $B^- \to J/\psi K^-$ and (right) $B^+ \to J/\psi K^+$ candidates with the result of the fit superimposed, for data collected at (top) 7 TeV and (bottom) 8 TeV, where the $B^\pm \to J/\psi \pi^\pm$ contributions are neglected.

Table 1: Signal yields and raw charge asymmetries determined from the fits, which are described in the text. The uncertainties are statistical.

	7 TeV	8 TeV
$N_{J/\psi\pi}$	6011 ± 89	$13\,103 \pm 130$
$N_{J/\psi K}$	$107\,783 \pm 332$	$243\,119 \pm 499$
$A^{\rm raw}_{J/\psi\pi}$	$(1.64 \pm 1.39) \times 10^{-2}$	$(1.35 \pm 0.94) \times 10^{-2}$
$A^{\rm raw}_{J/\psi K}$	$(-1.65 \pm 0.31) \times 10^{-2}$	$(-1.27 \pm 0.20) \times 10^{-2}$

5 Efficiency corrections

The ratio of the $B^+ \to J/\psi\pi^+$ and $B^+ \to J/\psi K^+$ branching fractions is measured separately for the 7 and 8 TeV samples, and is calculated as

$$\mathcal{R}_{\pi/K} = \frac{N_{J/\psi\pi}}{N_{J/\psi K}} \times \frac{\varepsilon_{J/\psi K}}{\varepsilon_{J/\psi\pi}}, \tag{3}$$

where $\varepsilon_{J/\psi\pi}$ and $\varepsilon_{J/\psi K}$ denote the total efficiencies of selecting the two modes, each taking into account the geometrical acceptance of the detector, the trigger, the reconstruction and preselection, the hadron PID, the BDT selection and the fiducial selection. The hadron

PID efficiencies are determined using $D^{*+} \to D^0(\to K^-\pi^+)\pi^+$ calibration data [25]. Kaons and pions in the calibration samples are weighted to reproduce the momentum and pseudorapidity distributions of those from $B^+ \to J/\psi K^+$ and $B^+ \to J/\psi \pi^+$ decays. All other efficiencies are estimated using simulated signal events. The simulated events are weighted such that their kinematic distributions match those of the background-subtracted data, which is obtained using the *sPlot* technique [26]. The efficiency ratio, $\varepsilon_{J/\psi\pi}/\varepsilon_{J/\psi K}$, is estimated to be 1.43 ± 0.01 for the 7 TeV data and 1.42 ± 0.01 for 8 TeV, with the difference from unity being mainly due to the PID selections for the two decays.

The difference in *CP* asymmetries of $B^+ \to J/\psi\pi^+$ and $B^+ \to J/\psi K^+$ is calculated as

$$\begin{aligned} \Delta\mathcal{A}^{CP} &= \Delta A^{\rm raw} - \Delta A^{\rm eff} , \\ \Delta A^{\rm raw} &\equiv A^{\rm raw}_{J/\psi\pi} - A^{\rm raw}_{J/\psi K} , \\ \Delta A^{\rm eff} &\equiv A^{\rm eff}_{J/\psi\pi} - A^{\rm eff}_{J/\psi K} , \end{aligned} \tag{4}$$

where $A^{\rm eff}_{J/\psi\pi}$ and $A^{\rm eff}_{J/\psi K}$ are the efficiency asymmetries between B^- and B^+ decays. The asymmetry difference $\Delta A^{\rm eff}$ arises from the particle detection efficiency, hadron PID, BDT selection and fiducial selection. The main sources of asymmetry are the detection efficiency and hadron PID, as described below.

The PID efficiency asymmetries of $B^+ \to J/\psi\pi^+$ and $B^+ \to J/\psi K^+$ are estimated separately using the $D^{*+} \to D^0(\to K^-\pi^+)\pi^+$ calibration sample mentioned above, and their difference is taken as a contribution to $\Delta A^{\rm eff}$. The average detection asymmetry between π^- and π^+ in $B^+ \to J/\psi\pi^+$ is denoted $A^{\rm det}_\pi$, and that between K^- and K^+ in $B^+ \to J/\psi K^+$ is likewise denoted $A^{\rm det}_K$. Following the method in Ref. [27], the difference $A^{\rm det}_\pi - A^{\rm det}_K$ can be approximated by the combined detection asymmetry between $\pi^- K^+$ and $\pi^+ K^-$, denoted $A^{\rm det}_{\pi\overline{K}}$, which is calculated as

$$A^{\rm det}_\pi - A^{\rm det}_K \approx A^{\rm det}_{\pi\overline{K}} = A^{\rm raw}_{D^-\to K^+\pi^-\pi^-} - A^{\rm raw}_{D^-\to K^0_{\rm S}\pi^-} + A^{\rm det}_{K^0_{\rm S}} . \tag{5}$$

Here $A^{\rm raw}_{D^-\to K^+\pi^-\pi^-}$ and $A^{\rm raw}_{D^-\to K^0_{\rm S}\pi^-}$ are the raw charge asymmetries measured in the decays $D^- \to K^+\pi^-\pi^-$ and $D^- \to K^0_{\rm S}\pi^-$. The $D^\mp$ production asymmetry cancels in the difference between the two raw asymmetries, and the *CP* asymmetries in Cabibbo-favoured charm decays are assumed to be negligible. The $D^- \to K^+\pi^-\pi^-$ decays are weighted to match the distributions of $p_{\rm T}$ and rapidity (y) of kaons in the $B^+ \to J/\psi K^+$ decays. The $D^- \to K^0_{\rm S}\pi^-$ decays are then weighted to match the kinematic distributions of the $D^- \to K^+\pi^-\pi^-$ sample such that the $p_{\rm T}$ and y distributions of the D^- agree between the two channels, as do the $p_{\rm T}$ distributions of the π^- (with one pion chosen at random in the case of $D^- \to K^+\pi^-\pi^-$). The term $A^{\rm det}_{K^0_{\rm S}}$ is a small correction for the effects of *CP* violation in K^0–$\overline{K}^0$ mixing and the different interaction cross-sections of K^0 and $\overline{K}^0$ with the detector material [28]. The asymmetry $A^{\rm det}_{\pi\overline{K}}$ is evaluated to be $(1.10 \pm 0.22) \times 10^{-2}$ and $(0.77 \pm 0.10) \times 10^{-2}$ for the 7 and 8 TeV data, respectively. The overall difference in efficiency asymmetry, $\Delta A^{\rm eff}$, is estimated to be $(1.37 \pm 0.56) \times 10^{-2}$ for the 7 TeV data, and $(0.84 \pm 0.43) \times 10^{-2}$ for 8 TeV.

6 Systematic uncertainties

The data-taking conditions were different for the 7 and 8 TeV data, and therefore the systematic uncertainties, summarised in Table 2, are computed separately for the two

samples. The relative uncertainties are quoted for the $\mathcal{R}_{\pi/K}$ measurement and absolute uncertainties are quoted for the $\Delta\mathcal{A}^{CP}$ measurement. The systematic uncertainties can be divided into two groups, either associated with the mass fit or with the efficiency. For each systematic uncertainty associated with the mass fit, a fit with an alternative model is performed and the differences in the mean values of $\mathcal{R}_{\pi/K}$ and $\Delta\mathcal{A}^{CP}$ are taken as the corresponding systematic uncertainties. In each case, the uncertainties are quoted separately for the 7 and 8 TeV data.

The baseline signal model is a Hypatia function. Changing this to a histogram representing the simulated signal mass distribution convolved with a Gaussian function, to correct for mismatch in resolution between data and simulation, leads to relative uncertainties of 0.39% and 0.25% for $\mathcal{R}_{\pi/K}$ for the 7 and 8 TeV data and absolute uncertainties of 0.03×10^{-2} and less than 0.01×10^{-2} for $\Delta\mathcal{A}^{CP}$.

The baseline model for the misidentification background in the $B^+ \to J/\psi\,\pi^+$ sample is a DSCB function with tail parameters obtained from the simulation. Alternative models are constructed by varying the tail parameter values to match those expected for different pion selection requirements, or by using a histogram convolved with a Gaussian function as was done for the signal model. The results from different alternative models are summed in quadrature. The resulting relative systematic uncertainties on $\mathcal{R}_{\pi/K}$ are 0.44% and 0.38%, and the estimated systematic uncertainties on $\Delta\mathcal{A}^{CP}$ are 0.01×10^{-2} and 0.02×10^{-2}.

The most probable values and the resolution parameters of the signal and misidentification background models are assumed to be the same for B^+ and B^- decays in the baseline fits. Treating the parameters separately for B^+ and B^- decays leads to differences (taken as estimates of the associated uncertainties) of 0.04×10^{-2} and 0.05×10^{-2} for $\Delta\mathcal{A}^{CP}$, while the effect on $\mathcal{R}_{\pi/K}$ is negligible.

The baseline model for the combinatorial background is an exponential function. Adding a linear component to this model shifts $\mathcal{R}_{\pi/K}$ by 0.52% and 0.20%, and changes $\Delta\mathcal{A}^{CP}$ by 0.04×10^{-2} and 0.01×10^{-2}.

The baseline fits are performed in mass ranges above $5000\,\mathrm{MeV}/c^2$, where contamination from the partially reconstructed background is expected up to $5150\,\mathrm{MeV}/c^2$. The alternative fits are performed in narrower ranges starting from $5150\,\mathrm{MeV}/c^2$, where partially reconstructed background can be neglected. The value of $\mathcal{R}_{\pi/K}$ is found to change by 0.20% and 0.33%, and that of $\Delta\mathcal{A}^{CP}$ by 0.04×10^{-2} and 0.01×10^{-2}. Systematic uncertainties equal to these shifts are assigned.

The PID efficiencies are calibrated using $D^{*+} \to D^0(\to K^-\pi^+)\pi^+$ decays selected without applying hadron PID requirements. The efficiency depends on the momentum and pseudorapidity of the track and the track multiplicity in the event, and the calibration is therefore done in bins of those variables. The choice of binning necessarily involves a compromise between the granularity and statistical uncertainty of individual bins. Systematic uncertainties due to the limited number of kinematic bins are evaluated by doubling or halving the number of bins and recalculating the average efficiencies. The resulting deviations from the baseline results are taken as the systematic uncertainties: 0.39% and 0.46% for $\mathcal{R}_{\pi/K}$, and 0.06×10^{-2} and 0.01×10^{-2} for $\Delta\mathcal{A}^{CP}$.

The ratio of BDT efficiencies of the decays $B^+ \to J/\psi\,\pi^+$ and $B^+ \to J/\psi\,K^+$ is estimated with simulated samples of signal events, which are weighted to remove differences in the distributions of the BDT input variables between the simulation and data. Relative systematic uncertainties of 0.01% and 0.02% are assigned to $\mathcal{R}_{\pi/K}$, to account for statistical uncertainties on the weights used in the efficiency calculation.

The ratio of trigger efficiencies of the decays $B^+ \to J/\psi\pi^+$ and $B^+ \to J/\psi K^+$ is determined from simulation and validated with a control sample of $J/\psi \to \mu^+\mu^-$ decays [12]. Relative differences of 0.33% and 0.38% are found between the values of this ratio estimated with data and with simulation, which are taken as the corresponding systematic uncertainties on $\mathcal{R}_{\pi/K}$.

Samples of D^+ decays are used to determine the difference between the kaon and pion detection efficiency asymmetries. However, the kinematic distributions of the pions and kaons in the D^+ samples may differ from those of the signal $B^+ \to J/\psi h^+$ samples, and the efficiency asymmetries may vary with the particle kinematics. To assess the scale of this effect, samples of $D^+ \to K^-\pi^+\pi^+$ events are weighted such that the distribution of the momentum of the kaon matches that of $B^+ \to J/\psi K^+$, leading to a pion detection asymmetry of 0.12×10^{-2} for both 7 and 8 TeV data. This is taken as a systematic uncertainty.

The production asymmetry of B^+ mesons is a function of the B^+ kinematics. This dependence cancels in the observables considered, provided that $B^+ \to J/\psi\pi^+$ and $B^+ \to J/\psi K^+$ decays have the same kinematic distributions. Good agreement is found between the $p_{\rm T}$ distributions of the decays $B^+ \to J/\psi\pi^+$ and $B^+ \to J/\psi K^+$, but not for the rapidity distributions. The deviations of the B^+ production asymmetry with and without the weights that match the rapidity distribution in the $B^+ \to J/\psi\pi^+$ sample to that of the $B^+ \to J/\psi K^+$ decay, are 0.02×10^{-2} and 0.04×10^{-2}, which are taken as the systematic uncertainties on $\Delta\mathcal{A}^{CP}$.

A systematic uncertainty of 0.03% on $\mathcal{R}_{\pi/K}$ is assigned to account for imperfect simulation of hadron interactions in the detector. Summing all of the above contributions in quadrature, the relative systematic uncertainty on $\mathcal{R}_{\pi/K}$ is 1.01% for the 7 TeV sample and 0.83% for 8 TeV and the absolute uncertainty on $\Delta\mathcal{A}^{CP}$ is 0.15×10^{-2} for 7 TeV and 0.14×10^{-2} for 8 TeV.

7 Results and conclusion

Using the estimated signal yields, efficiency ratios, raw charge asymmetries and efficiency asymmetries, the ratio of branching fractions and difference in *CP* asymmetries of the decay modes $B^+ \to J/\psi\pi^+$ and $B^+ \to J/\psi K^+$ are measured to be

$$\mathcal{R}_{\pi/K} = \begin{cases} (3.90 \pm 0.06 \pm 0.04) \times 10^{-2} & \text{for 7 TeV} \\ (3.79 \pm 0.04 \pm 0.03) \times 10^{-2} & \text{for 8 TeV}\,, \end{cases}$$

$$\Delta\mathcal{A}^{CP} = \begin{cases} (1.92 \pm 1.53 \pm 0.15) \times 10^{-2} & \text{for 7 TeV} \\ (1.77 \pm 1.05 \pm 0.14) \times 10^{-2} & \text{for 8 TeV}\,. \end{cases}$$

Here the first uncertainties are statistical, which are uncorrelated between the 7 and 8 TeV results, and the second uncertainties are systematic, which are taken to be fully correlated between the 7 and 8 TeV results. The average of the 7 and 8 TeV results, weighting each according to its statistical uncertainty, are

$$\mathcal{R}_{\pi/K} = (3.83 \pm 0.03 \pm 0.03) \times 10^{-2},$$
$$\Delta\mathcal{A}^{CP} = (1.82 \pm 0.86 \pm 0.14) \times 10^{-2}.$$

Table 2: Relative systematic uncertainties (%) for $\mathcal{R}_{\pi/K}$ and absolute systematic uncertainties ($\times 10^{-2}$) for $\Delta\mathcal{A}^{CP}$. The uncertainties are quoted separately for the 7 and 8 TeV data. The dashes indicate negligible uncertainties (zero after rounding to two decimal places).

Sources	$\mathcal{R}_{\pi/K}$ (7 TeV) [%]	$\mathcal{R}_{\pi/K}$ (8 TeV) [%]	$\Delta\mathcal{A}^{CP}$ (7 TeV) [$\times 10^{-2}$]	$\Delta\mathcal{A}^{CP}$ (8 TeV) [$\times 10^{-2}$]
Signal model	0.39	0.25	0.03	–
Mis-ID background	0.44	0.38	0.01	0.02
$B^{\pm}$ parameters	0.04	0.02	0.04	0.05
Comb. background	0.52	0.20	0.04	0.01
Part. reco. background	0.20	0.33	0.04	0.01
PID efficiency	0.39	0.46	0.06	0.01
BDT efficiency	0.01	0.02	–	–
Trigger efficiency	0.33	0.38	–	–
Detection asymmetry	–	–	0.12	0.12
$B^{\pm}$ prod. asymmetry	–	–	0.02	0.04
K/π interaction	0.03	0.03	–	–
Total	1.01	0.83	0.15	0.14

The LHCb collaboration has recently reported the *CP* asymmetry $\mathcal{A}^{CP}(B^+ \to J/\psi K^+) = (0.09 \pm 0.27 \pm 0.07) \times 10^{-2}$ [9], where the first uncertainty is statistical and the second systematic. The sample analysed in Ref. [9] is statistically correlated with that used in this analysis, but the correlation is only partial due to the use of different trigger requirements. The correlation coefficient between the statistical uncertainties of the two analyses is found to be -4.8%. The systematic uncertainty on $\mathcal{A}^{CP}(B^+ \to J/\psi K^+)$ is taken to be uncorrelated with that on the $\Delta\mathcal{A}^{CP}$ measurement. Therefore the *CP* asymmetry in the decay $B^+ \to J/\psi \pi^+$ is

$$\mathcal{A}^{CP}(B^+ \to J/\psi \pi^+) = \Delta\mathcal{A}^{CP} + \mathcal{A}^{CP}(B^+ \to J/\psi K^+) = (1.91 \pm 0.89 \pm 0.16) \times 10^{-2}.$$

This is the most precise determination of $\mathcal{A}^{CP}(B^+ \to J/\psi \pi^+)$ to date, and it supersedes the previous LHCb result [8]. The $\mathcal{R}_{\pi/K}$ and $\mathcal{A}^{CP}(B^+ \to J/\psi \pi^+)$ measurements can be combined with measurements of decay rates and *CP* asymmetries in other $b \to c\bar{c}d$ decays, such as $B^0 \to J/\psi \pi^0$, to understand the effect of loop contributions in $b \to c\bar{c}s$ decays using SU(3) flavour symmetry [2, 3].

Acknowledgements

We express our gratitude to our colleagues in the CERN accelerator departments for the excellent performance of the LHC. We thank the technical and administrative staff at the LHCb institutes. We acknowledge support from CERN and from the national agencies: CAPES, CNPq, FAPERJ and FINEP (Brazil); NSFC (China); CNRS/IN2P3 (France); BMBF, DFG and MPG (Germany); INFN (Italy); FOM and NWO (The Netherlands); MNiSW and NCN (Poland); MEN/IFA (Romania); MinES and FASO (Russia); MinECo (Spain); SNSF and SER (Switzerland); NASU (Ukraine); STFC (United Kingdom); NSF

(USA). We acknowledge the computing resources that are provided by CERN, IN2P3 (France), KIT and DESY (Germany), INFN (Italy), SURF (The Netherlands), PIC (Spain), GridPP (United Kingdom), RRCKI and Yandex LLC (Russia), CSCS (Switzerland), IFIN-HH (Romania), CBPF (Brazil), PL-GRID (Poland) and OSC (USA). We are indebted to the communities behind the multiple open source software packages on which we depend. Individual groups or members have received support from AvH Foundation (Germany), EPLANET, Marie Skłodowska-Curie Actions and ERC (European Union), Conseil Général de Haute-Savoie, Labex ENIGMASS and OCEVU, Région Auvergne (France), RFBR and Yandex LLC (Russia), GVA, XuntaGal and GENCAT (Spain), Herchel Smith Fund, The Royal Society, Royal Commission for the Exhibition of 1851 and the Leverhulme Trust (United Kingdom).

References

[1] I. Dunietz and J. M. Soares, *Direct CP violation in $b \to dJ/\psi$ decays*, Phys. Rev. **D49** (1994) 5904, arXiv:hep-ph/9312233.

[2] Z. Ligeti and D. J. Robinson, *Towards more precise determinations of the quark mixing phase β*, Phys. Rev. Lett. **115** (2015) 251801, arXiv:1507.06671.

[3] K. De Bruyn and R. Fleischer, *A roadmap to control penguin effects in $B^0_d \to J/\psi\, K^0_{\rm S}$ and $B^0_s \to J/\psi\,\phi$*, JHEP **03** (2015) 145, arXiv:1412.6834.

[4] Particle Data Group, C. Patrignani *et al.*, *Review of particle physics*, Chin. Phys. **C40** (2016) 100001.

[5] Belle collaboration, K. Abe *et al.*, *Measurement of branching fractions and charge asymmetries for two-body B meson decays with charmonium*, Phys. Rev. **D67** (2003) 032003, arXiv:hep-ex/0211047.

[6] BaBar collaboration, B. Aubert *et al.*, *Study of $B^\pm \to J/\psi\,\pi^\pm$ and $B^\pm \to J/\psi\, K^\pm$ decays: Measurement of the ratio of branching fractions and search for direct CP violation*, Phys. Rev. Lett. **92** (2004) 241802, arXiv:hep-ex/0401035.

[7] D0 collaboration, V. M. Abazov *et al.*, *Measurement of direct CP violation parameters in $B^\pm \to J/\psi\, K^\pm$ and $B^\pm \to J/\psi\,\pi^\pm$ decays with $10.4\,fb^{-1}$ of Tevatron data*, Phys. Rev. Lett. **110** (2013) 241801, arXiv:1304.1655.

[8] LHCb collaboration, R. Aaij *et al.*, *Measurements of the branching fractions and CP asymmetries of $B^\pm \to J/\psi\,\pi^\pm$ and $B^\pm \to \psi(2S)\pi^\pm$ decays*, Phys. Rev. **D85** (2012) 091105(R), arXiv:1203.3592.

[9] LHCb collaboration, R. Aaij *et al.*, *B^+ production asymmetry and $\mathcal{A}^{CP}(B^+ \to J/\psi K^+)$*, LHCb-PAPER-2016-054, in preparation.

[10] LHCb collaboration, A. A. Alves Jr. *et al.*, *The LHCb detector at the LHC*, JINST **3** (2008) S08005.

[11] LHCb collaboration, R. Aaij *et al.*, *LHCb detector performance*, Int. J. Mod. Phys. **A30** (2015) 1530022, arXiv:1412.6352.

[12] R. Aaij *et al.*, *The LHCb trigger and its performance in 2011*, JINST **8** (2013) P04022, arXiv:1211.3055.

[13] T. Sjöstrand, S. Mrenna, and P. Skands, *PYTHIA 6.4 physics and manual*, JHEP **05** (2006) 026, arXiv:hep-ph/0603175.

[14] T. Sjöstrand, S. Mrenna, and P. Skands, *A brief introduction to PYTHIA 8.1*, Comput. Phys. Commun. **178** (2008) 852, arXiv:0710.3820.

[15] I. Belyaev *et al.*, *Handling of the generation of primary events in Gauss, the LHCb simulation framework*, J. Phys. Conf. Ser. **331** (2011) 032047.

[16] D. J. Lange, *The EvtGen particle decay simulation package*, Nucl. Instrum. Meth. **A462** (2001) 152.

[17] P. Golonka and Z. Was, *PHOTOS Monte Carlo: A precision tool for QED corrections in Z and W decays*, Eur. Phys. J. **C45** (2006) 97, arXiv:hep-ph/0506026.

[18] Geant4 collaboration, J. Allison *et al.*, *Geant4 developments and applications*, IEEE Trans. Nucl. Sci. **53** (2006) 270; Geant4 collaboration, S. Agostinelli *et al.*, *Geant4: A simulation toolkit*, Nucl. Instrum. Meth. **A506** (2003) 250.

[19] M. Clemencic *et al.*, *The LHCb simulation application, Gauss: Design, evolution and experience*, J. Phys. Conf. Ser. **331** (2011) 032023.

[20] L. Breiman, J. H. Friedman, R. A. Olshen, and C. J. Stone, *Classification and regression trees*, Wadsworth international group, Belmont, California, USA, 1984.

[21] Y. Freund and R. E. Schapire, *A decision-theoretic generalization of on-line learning and an application to boosting*, J. Comput. Syst. Sci. **55** (1997) 119.

[22] D. Martínez Santos and F. Dupertuis, *Mass distributions marginalized over per-event errors*, Nucl. Instrum. Meth. **A764** (2014) 150, arXiv:1312.5000.

[23] ARGUS collaboration, H. Albrecht *et al.*, *Search for hadronic $b \to u$ decays*, Phys. Lett. **B241** (1990) 278.

[24] LHCb collaboration, R. Aaij *et al.*, *First observation of the decay $B^+ \to \pi^+\mu^+\mu^-$*, JHEP **12** (2012) 125, arXiv:1210.2645.

[25] L. Anderlini *et al.*, *The PIDCalib package*, CERN-LHCb-PUB-2016-021.

[26] M. Pivk and F. R. Le Diberder, *sPlot: A statistical tool to unfold data distributions*, Nucl. Instrum. Meth. **A555** (2005) 356, arXiv:physics/0402083.

[27] LHCb collaboration, R. Aaij *et al.*, *Measurement of indirect CP asymmetries in $D^0 \to K^-K^+$ and $D^0 \to \pi^-\pi^+$ decays*, JHEP **04** (2015) 043, arXiv:1501.06777.

[28] LHCb collaboration, R. Aaij *et al.*, *Measurement of CP asymmetry in $D^0 \to K^-K^+$ and $D^0 \to \pi^-\pi^+$ decays*, JHEP **07** (2014) 041, arXiv:1405.2797.

LHCb collaboration

R. Aaij[40], B. Adeva[39], M. Adinolfi[48], Z. Ajaltouni[5], S. Akar[59], J. Albrecht[10], F. Alessio[40], M. Alexander[53], S. Ali[43], G. Alkhazov[31], P. Alvarez Cartelle[55], A.A. Alves Jr[59], S. Amato[2], S. Amerio[23], Y. Amhis[7], L. An[3], L. Anderlini[18], G. Andreassi[41], M. Andreotti[17,g], J.E. Andrews[60], R.B. Appleby[56], F. Archilli[43], P. d'Argent[12], J. Arnau Romeu[6], A. Artamonov[37], M. Artuso[61], E. Aslanides[6], G. Auriemma[26], M. Baalouch[5], I. Babuschkin[56], S. Bachmann[12], J.J. Back[50], A. Badalov[38], C. Baesso[62], S. Baker[55], V. Balagura[7,c], W. Baldini[17], R.J. Barlow[56], C. Barschel[40], S. Barsuk[7], W. Barter[40], M. Baszczyk[27], V. Batozskaya[29], B. Batsukh[61], V. Battista[41], A. Bay[41], L. Beaucourt[4], J. Beddow[53], F. Bedeschi[24], I. Bediaga[1], L.J. Bel[43], V. Bellee[41], N. Belloli[21,i], K. Belous[37], I. Belyaev[32], E. Ben-Haim[8], G. Bencivenni[19], S. Benson[43], A. Berezhnoy[33], R. Bernet[42], A. Bertolin[23], C. Betancourt[42], F. Betti[15], M.-O. Bettler[40], M. van Beuzekom[43], Ia. Bezshyiko[42], S. Bifani[47], P. Billoir[8], T. Bird[56], A. Birnkraut[10], A. Bitadze[56], A. Bizzeti[18,u], T. Blake[50], F. Blanc[41], J. Blouw[11,†], S. Blusk[61], V. Bocci[26], T. Boettcher[58], A. Bondar[36,w], N. Bondar[31,40], W. Bonivento[16], I. Bordyuzhin[32], A. Borgheresi[21,i], S. Borghi[56], M. Borisyak[35], M. Borsato[39], F. Bossu[7], M. Boubdir[9], T.J.V. Bowcock[54], E. Bowen[42], C. Bozzi[17,40], S. Braun[12], M. Britsch[12], T. Britton[61], J. Brodzicka[56], E. Buchanan[48], C. Burr[56], A. Bursche[2], J. Buytaert[40], S. Cadeddu[16], R. Calabrese[17,g], M. Calvi[21,i], M. Calvo Gomez[38,m], A. Camboni[38], P. Campana[19], D.H. Campora Perez[40], L. Capriotti[56], A. Carbone[15,e], G. Carboni[25,j], R. Cardinale[20,h], A. Cardini[16], P. Carniti[21,i], L. Carson[52], K. Carvalho Akiba[2], G. Casse[54], L. Cassina[21,i], L. Castillo Garcia[41], M. Cattaneo[40], G. Cavallero[20], R. Cenci[24,t], D. Chamont[7], M. Charles[8], Ph. Charpentier[40], G. Chatzikonstantinidis[47], M. Chefdeville[4], S. Chen[56], S.-F. Cheung[57], V. Chobanova[39], M. Chrzaszcz[42,27], X. Cid Vidal[39], G. Ciezarek[43], P.E.L. Clarke[52], M. Clemencic[40], H.V. Cliff[49], J. Closier[40], V. Coco[59], J. Cogan[6], E. Cogneras[5], V. Cogoni[16,40,f], L. Cojocariu[30], G. Collazuol[23,o], P. Collins[40], A. Comerma-Montells[12], A. Contu[40], A. Cook[48], G. Coombs[40], S. Coquereau[38], G. Corti[40], M. Corvo[17,g], C.M. Costa Sobral[50], B. Couturier[40], G.A. Cowan[52], D.C. Craik[52], A. Crocombe[50], M. Cruz Torres[62], S. Cunliffe[55], R. Currie[55], C. D'Ambrosio[40], F. Da Cunha Marinho[2], E. Dall'Occo[43], J. Dalseno[48], P.N.Y. David[43], A. Davis[3], K. De Bruyn[6], S. De Capua[56], M. De Cian[12], J.M. De Miranda[1], L. De Paula[2], M. De Serio[14,d], P. De Simone[19], C.-T. Dean[53], D. Decamp[4], M. Deckenhoff[10], L. Del Buono[8], M. Demmer[10], A. Dendek[28], D. Derkach[35], O. Deschamps[5], F. Dettori[40], B. Dey[22], A. Di Canto[40], H. Dijkstra[40], F. Dordei[40], M. Dorigo[41], A. Dosil Suárez[39], A. Dovbnya[45], K. Dreimanis[54], L. Dufour[43], G. Dujany[56], K. Dungs[40], P. Durante[40], R. Dzhelyadin[37], A. Dziurda[40], A. Dzyuba[31], N. Déléage[4], S. Easo[51], M. Ebert[52], U. Egede[55], V. Egorychev[32], S. Eidelman[36,w], S. Eisenhardt[52], U. Eitschberger[10], R. Ekelhof[10], L. Eklund[53], S. Ely[61], S. Esen[12], H.M. Evans[49], T. Evans[57], A. Falabella[15], N. Farley[47], S. Farry[54], R. Fay[54], D. Fazzini[21,i], D. Ferguson[52], A. Fernandez Prieto[39], F. Ferrari[15,40], F. Ferreira Rodrigues[2], M. Ferro-Luzzi[40], S. Filippov[34], R.A. Fini[14], M. Fiore[17,g], M. Fiorini[17,g], M. Firlej[28], C. Fitzpatrick[41], T. Fiutowski[28], F. Fleuret[7,b], K. Fohl[40], M. Fontana[16,40], F. Fontanelli[20,h], D.C. Forshaw[61], R. Forty[40], V. Franco Lima[54], M. Frank[40], C. Frei[40], J. Fu[22,q], W. Funk[40], E. Furfaro[25,j], C. Färber[40], A. Gallas Torreira[39], D. Galli[15,e], S. Gallorini[23], S. Gambetta[52], M. Gandelman[2], P. Gandini[57], Y. Gao[3], L.M. Garcia Martin[69], J. García Pardiñas[39], J. Garra Tico[49], L. Garrido[38], P.J. Garsed[49], D. Gascon[38], C. Gaspar[40], L. Gavardi[10], G. Gazzoni[5], D. Gerick[12], E. Gersabeck[12], M. Gersabeck[56], T. Gershon[50], Ph. Ghez[4], S. Gianì[41], V. Gibson[49], O.G. Girard[41], L. Giubega[30], K. Gizdov[52], V.V. Gligorov[8], D. Golubkov[32], A. Golutvin[55,40], A. Gomes[1,a], I.V. Gorelov[33], C. Gotti[21,i], R. Graciani Diaz[38], L.A. Granado Cardoso[40], E. Graugés[38], E. Graverini[42], G. Graziani[18], A. Grecu[30], P. Griffith[47], L. Grillo[21,40,i], B.R. Gruberg Cazon[57], O. Grünberg[67], E. Gushchin[34], Yu. Guz[37], T. Gys[40], C. Göbel[62], T. Hadavizadeh[57], C. Hadjivasiliou[5], G. Haefeli[41], C. Haen[40], S.C. Haines[49],

S. Hall[55], B. Hamilton[60], X. Han[12], S. Hansmann-Menzemer[12], N. Harnew[57], S.T. Harnew[48], J. Harrison[56], M. Hatch[40], J. He[63], T. Head[41], A. Heister[9], K. Hennessy[54], P. Henrard[5], L. Henry[8], E. van Herwijnen[40], M. Heß[67], A. Hicheur[2], D. Hill[57], C. Hombach[56], H. Hopchev[41], W. Hulsbergen[43], T. Humair[55], M. Hushchyn[35], D. Hutchcroft[54], M. Idzik[28], P. Ilten[58], R. Jacobsson[40], A. Jaeger[12], J. Jalocha[57], E. Jans[43], A. Jawahery[60], F. Jiang[3], M. John[57], D. Johnson[40], C.R. Jones[49], C. Joram[40], B. Jost[40], N. Jurik[57], S. Kandybei[45], M. Karacson[40], J.M. Kariuki[48], S. Karodia[53], M. Kecke[12], M. Kelsey[61], M. Kenzie[49], T. Ketel[44], E. Khairullin[35], B. Khanji[12], C. Khurewathanakul[41], T. Kirn[9], S. Klaver[56], K. Klimaszewski[29], S. Koliiev[46], M. Kolpin[12], I. Komarov[41], R.F. Koopman[44], P. Koppenburg[43], A. Kosmyntseva[32], A. Kozachuk[33], M. Kozeiha[5], L. Kravchuk[34], K. Kreplin[12], M. Kreps[50], P. Krokovny[36,w], F. Kruse[10], W. Krzemien[29], W. Kucewicz[27,l], M. Kucharczyk[27], V. Kudryavtsev[36,w], A.K. Kuonen[41], K. Kurek[29], T. Kvaratskheliya[32,40], D. Lacarrere[40], G. Lafferty[56], A. Lai[16], G. Lanfranchi[19], C. Langenbruch[9], T. Latham[50], C. Lazzeroni[47], R. Le Gac[6], J. van Leerdam[43], A. Leflat[33,40], J. Lefrançois[7], R. Lefèvre[5], F. Lemaitre[40], E. Lemos Cid[39], O. Leroy[6], T. Lesiak[27], B. Leverington[12], T. Li[3], Y. Li[7], T. Likhomanenko[35,68], R. Lindner[40], C. Linn[40], F. Lionetto[42], X. Liu[3], D. Loh[50], I. Longstaff[53], J.H. Lopes[2], D. Lucchesi[23,o], M. Lucio Martinez[39], H. Luo[52], A. Lupato[23], E. Luppi[17,g], O. Lupton[40], A. Lusiani[24], X. Lyu[63], F. Machefert[7], F. Maciuc[30], O. Maev[31], K. Maguire[56], S. Malde[57], A. Malinin[68], T. Maltsev[36], G. Manca[16,f], G. Mancinelli[6], P. Manning[61], J. Maratas[5,v], J.F. Marchand[4], U. Marconi[15], C. Marin Benito[38], M. Marinangeli[41], P. Marino[24,t], J. Marks[12], G. Martellotti[26], M. Martin[6], M. Martinelli[41], D. Martinez Santos[39], F. Martinez Vidal[69], D. Martins Tostes[2], L.M. Massacrier[7], A. Massafferri[1], R. Matev[40], A. Mathad[50], Z. Mathe[40], C. Matteuzzi[21], A. Mauri[42], E. Maurice[7,b], B. Maurin[41], A. Mazurov[47], M. McCann[55,40], A. McNab[56], R. McNulty[13], B. Meadows[59], F. Meier[10], M. Meissner[12], D. Melnychuk[29], M. Merk[43], A. Merli[22,q], E. Michielin[23], D.A. Milanes[66], M.-N. Minard[4], D.S. Mitzel[12], A. Mogini[8], J. Molina Rodriguez[1], I.A. Monroy[66], S. Monteil[5], M. Morandin[23], P. Morawski[28], A. Mordà[6], M.J. Morello[24,t], O. Morgunova[68], J. Moron[28], A.B. Morris[52], R. Mountain[61], F. Muheim[52], M. Mulder[43], M. Mussini[15], D. Müller[56], J. Müller[10], K. Müller[42], V. Müller[10], P. Naik[48], T. Nakada[41], R. Nandakumar[51], A. Nandi[57], I. Nasteva[2], M. Needham[52], N. Neri[22], S. Neubert[12], N. Neufeld[40], M. Neuner[12], T.D. Nguyen[41], C. Nguyen-Mau[41,n], S. Nieswand[9], R. Niet[10], N. Nikitin[33], T. Nikodem[12], A. Nogay[68], A. Novoselov[37], D.P. O'Hanlon[50], A. Oblakowska-Mucha[28], V. Obraztsov[37], S. Ogilvy[19], R. Oldeman[16,f], C.J.G. Onderwater[70], J.M. Otalora Goicochea[2], A. Otto[40], P. Owen[42], A. Oyanguren[69], P.R. Pais[41], A. Palano[14,d], F. Palombo[22,q], M. Palutan[19], A. Papanestis[51], M. Pappagallo[14,d], L.L. Pappalardo[17,g], W. Parker[60], C. Parkes[56], G. Passaleva[18], A. Pastore[14,d], G.D. Patel[54], M. Patel[55], C. Patrignani[15,e], A. Pearce[40], A. Pellegrino[43], G. Penso[26], M. Pepe Altarelli[40], S. Perazzini[40], P. Perret[5], L. Pescatore[47], K. Petridis[48], A. Petrolini[20,h], A. Petrov[68], M. Petruzzo[22,q], E. Picatoste Olloqui[38], B. Pietrzyk[4], M. Pikies[27], D. Pinci[26], A. Pistone[20], A. Piucci[12], V. Placinta[30], S. Playfer[52], M. Plo Casasus[39], T. Poikela[40], F. Polci[8], A. Poluektov[50,36], I. Polyakov[61], E. Polycarpo[2], G.J. Pomery[48], A. Popov[37], D. Popov[11,40], B. Popovici[30], S. Poslavskii[37], C. Potterat[2], E. Price[48], J.D. Price[54], J. Prisciandaro[39,40], A. Pritchard[54], C. Prouve[48], V. Pugatch[46], A. Puig Navarro[42], G. Punzi[24,p], W. Qian[50], R. Quagliani[7,48], B. Rachwal[27], J.H. Rademacker[48], M. Rama[24], M. Ramos Pernas[39], M.S. Rangel[2], I. Raniuk[45], F. Ratnikov[35], G. Raven[44], F. Redi[55], S. Reichert[10], A.C. dos Reis[1], C. Remon Alepuz[69], V. Renaudin[7], S. Ricciardi[51], S. Richards[48], M. Rihl[40], K. Rinnert[54], V. Rives Molina[38], P. Robbe[7,40], A.B. Rodrigues[1], E. Rodrigues[59], J.A. Rodriguez Lopez[66], P. Rodriguez Perez[56,†], A. Rogozhnikov[35], S. Roiser[40], A. Rollings[57], V. Romanovskiy[37], A. Romero Vidal[39], J.W. Ronayne[13], M. Rotondo[19], M.S. Rudolph[61], T. Ruf[40], P. Ruiz Valls[69], J.J. Saborido Silva[39], E. Sadykhov[32], N. Sagidova[31], B. Saitta[16,f], V. Salustino Guimaraes[1], C. Sanchez Mayordomo[69], B. Sanmartin Sedes[39], R. Santacesaria[26], C. Santamarina Rios[39],

M. Santimaria[19], E. Santovetti[25,j], A. Sarti[19,k], C. Satriano[26,s], A. Satta[25], D.M. Saunders[48], D. Savrina[32,33], S. Schael[9], M. Schellenberg[10], M. Schiller[53], H. Schindler[40], M. Schlupp[10], M. Schmelling[11], T. Schmelzer[10], B. Schmidt[40], O. Schneider[41], A. Schopper[40], K. Schubert[10], M. Schubiger[41], M.-H. Schune[7], R. Schwemmer[40], B. Sciascia[19], A. Sciubba[26,k], A. Semennikov[32], A. Sergi[47], N. Serra[42], J. Serrano[6], L. Sestini[23], P. Seyfert[21], M. Shapkin[37], I. Shapoval[45], Y. Shcheglov[31], T. Shears[54], L. Shekhtman[36,w], V. Shevchenko[68], B.G. Siddi[17,40], R. Silva Coutinho[42], L. Silva de Oliveira[2], G. Simi[23,o], S. Simone[14,d], M. Sirendi[49], N. Skidmore[48], T. Skwarnicki[61], E. Smith[55], I.T. Smith[52], J. Smith[49], M. Smith[55], H. Snoek[43], l. Soares Lavra[1], M.D. Sokoloff[59], F.J.P. Soler[53], B. Souza De Paula[2], B. Spaan[10], P. Spradlin[53], S. Sridharan[40], F. Stagni[40], M. Stahl[12], S. Stahl[40], P. Stefko[41], S. Stefkova[55], O. Steinkamp[42], S. Stemmle[12], O. Stenyakin[37], H. Stevens[10], S. Stevenson[57], S. Stoica[30], S. Stone[61], B. Storaci[42], S. Stracka[24,p], M. Straticiuc[30], U. Straumann[42], L. Sun[64], W. Sutcliffe[55], K. Swientek[28], V. Syropoulos[44], M. Szczekowski[29], T. Szumlak[28], S. T'Jampens[4], A. Tayduganov[6], T. Tekampe[10], G. Tellarini[17,g], F. Teubert[40], E. Thomas[40], J. van Tilburg[43], M.J. Tilley[55], V. Tisserand[4], M. Tobin[41], S. Tolk[49], L. Tomassetti[17,g], D. Tonelli[40], S. Topp-Joergensen[57], F. Toriello[61], E. Tournefier[4], S. Tourneur[41], K. Trabelsi[41], M. Traill[53], M.T. Tran[41], M. Tresch[42], A. Trisovic[40], A. Tsaregorodtsev[6], P. Tsopelas[43], A. Tully[49], N. Tuning[43], A. Ukleja[29], A. Ustyuzhanin[35], U. Uwer[12], C. Vacca[16,f], V. Vagnoni[15,40], A. Valassi[40], S. Valat[40], G. Valenti[15], R. Vazquez Gomez[19], P. Vazquez Regueiro[39], S. Vecchi[17], M. van Veghel[43], J.J. Velthuis[48], M. Veltri[18,r], G. Veneziano[57], A. Venkateswaran[61], M. Vernet[5], M. Vesterinen[12], J.V. Viana Barbosa[40], B. Viaud[7], D. Vieira[63], M. Vieites Diaz[39], H. Viemann[67], X. Vilasis-Cardona[38,m], M. Vitti[49], V. Volkov[33], A. Vollhardt[42], B. Voneki[40], A. Vorobyev[31], V. Vorobyev[36,w], C. Voß[9], J.A. de Vries[43], C. Vázquez Sierra[39], R. Waldi[67], C. Wallace[50], R. Wallace[13], J. Walsh[24], J. Wang[61], D.R. Ward[49], H.M. Wark[54], N.K. Watson[47], D. Websdale[55], A. Weiden[42], M. Whitehead[40], J. Wicht[50], G. Wilkinson[57,40], M. Wilkinson[61], M. Williams[40], M.P. Williams[47], M. Williams[58], T. Williams[47], F.F. Wilson[51], J. Wimberley[60], J. Wishahi[10], W. Wislicki[29], M. Witek[27], G. Wormser[7], S.A. Wotton[49], K. Wraight[53], K. Wyllie[40], Y. Xie[65], Z. Xing[61], Z. Xu[41], Z. Yang[3], Y. Yao[61], H. Yin[65], J. Yu[65], X. Yuan[36,w], O. Yushchenko[37], K.A. Zarebski[47], M. Zavertyaev[11,c], L. Zhang[3], Y. Zhang[7], Y. Zhang[63], A. Zhelezov[12], Y. Zheng[63], X. Zhu[3], V. Zhukov[33], S. Zucchelli[15].

[1] *Centro Brasileiro de Pesquisas Físicas (CBPF), Rio de Janeiro, Brazil*
[2] *Universidade Federal do Rio de Janeiro (UFRJ), Rio de Janeiro, Brazil*
[3] *Center for High Energy Physics, Tsinghua University, Beijing, China*
[4] *LAPP, Université Savoie Mont-Blanc, CNRS/IN2P3, Annecy-Le-Vieux, France*
[5] *Clermont Université, Université Blaise Pascal, CNRS/IN2P3, LPC, Clermont-Ferrand, France*
[6] *CPPM, Aix-Marseille Université, CNRS/IN2P3, Marseille, France*
[7] *LAL, Université Paris-Sud, CNRS/IN2P3, Orsay, France*
[8] *LPNHE, Université Pierre et Marie Curie, Université Paris Diderot, CNRS/IN2P3, Paris, France*
[9] *I. Physikalisches Institut, RWTH Aachen University, Aachen, Germany*
[10] *Fakultät Physik, Technische Universität Dortmund, Dortmund, Germany*
[11] *Max-Planck-Institut für Kernphysik (MPIK), Heidelberg, Germany*
[12] *Physikalisches Institut, Ruprecht-Karls-Universität Heidelberg, Heidelberg, Germany*
[13] *School of Physics, University College Dublin, Dublin, Ireland*
[14] *Sezione INFN di Bari, Bari, Italy*
[15] *Sezione INFN di Bologna, Bologna, Italy*
[16] *Sezione INFN di Cagliari, Cagliari, Italy*
[17] *Sezione INFN di Ferrara, Ferrara, Italy*
[18] *Sezione INFN di Firenze, Firenze, Italy*
[19] *Laboratori Nazionali dell'INFN di Frascati, Frascati, Italy*
[20] *Sezione INFN di Genova, Genova, Italy*
[21] *Sezione INFN di Milano Bicocca, Milano, Italy*
[22] *Sezione INFN di Milano, Milano, Italy*

[23] *Sezione INFN di Padova, Padova, Italy*
[24] *Sezione INFN di Pisa, Pisa, Italy*
[25] *Sezione INFN di Roma Tor Vergata, Roma, Italy*
[26] *Sezione INFN di Roma La Sapienza, Roma, Italy*
[27] *Henryk Niewodniczanski Institute of Nuclear Physics Polish Academy of Sciences, Kraków, Poland*
[28] *AGH - University of Science and Technology, Faculty of Physics and Applied Computer Science, Kraków, Poland*
[29] *National Center for Nuclear Research (NCBJ), Warsaw, Poland*
[30] *Horia Hulubei National Institute of Physics and Nuclear Engineering, Bucharest-Magurele, Romania*
[31] *Petersburg Nuclear Physics Institute (PNPI), Gatchina, Russia*
[32] *Institute of Theoretical and Experimental Physics (ITEP), Moscow, Russia*
[33] *Institute of Nuclear Physics, Moscow State University (SINP MSU), Moscow, Russia*
[34] *Institute for Nuclear Research of the Russian Academy of Sciences (INR RAN), Moscow, Russia*
[35] *Yandex School of Data Analysis, Moscow, Russia*
[36] *Budker Institute of Nuclear Physics (SB RAS), Novosibirsk, Russia*
[37] *Institute for High Energy Physics (IHEP), Protvino, Russia*
[38] *ICCUB, Universitat de Barcelona, Barcelona, Spain*
[39] *Universidad de Santiago de Compostela, Santiago de Compostela, Spain*
[40] *European Organization for Nuclear Research (CERN), Geneva, Switzerland*
[41] *Institute of Physics, Ecole Polytechnique Fédérale de Lausanne (EPFL), Lausanne, Switzerland*
[42] *Physik-Institut, Universität Zürich, Zürich, Switzerland*
[43] *Nikhef National Institute for Subatomic Physics, Amsterdam, The Netherlands*
[44] *Nikhef National Institute for Subatomic Physics and VU University Amsterdam, Amsterdam, The Netherlands*
[45] *NSC Kharkiv Institute of Physics and Technology (NSC KIPT), Kharkiv, Ukraine*
[46] *Institute for Nuclear Research of the National Academy of Sciences (KINR), Kyiv, Ukraine*
[47] *University of Birmingham, Birmingham, United Kingdom*
[48] *H.H. Wills Physics Laboratory, University of Bristol, Bristol, United Kingdom*
[49] *Cavendish Laboratory, University of Cambridge, Cambridge, United Kingdom*
[50] *Department of Physics, University of Warwick, Coventry, United Kingdom*
[51] *STFC Rutherford Appleton Laboratory, Didcot, United Kingdom*
[52] *School of Physics and Astronomy, University of Edinburgh, Edinburgh, United Kingdom*
[53] *School of Physics and Astronomy, University of Glasgow, Glasgow, United Kingdom*
[54] *Oliver Lodge Laboratory, University of Liverpool, Liverpool, United Kingdom*
[55] *Imperial College London, London, United Kingdom*
[56] *School of Physics and Astronomy, University of Manchester, Manchester, United Kingdom*
[57] *Department of Physics, University of Oxford, Oxford, United Kingdom*
[58] *Massachusetts Institute of Technology, Cambridge, MA, United States*
[59] *University of Cincinnati, Cincinnati, OH, United States*
[60] *University of Maryland, College Park, MD, United States*
[61] *Syracuse University, Syracuse, NY, United States*
[62] *Pontifícia Universidade Católica do Rio de Janeiro (PUC-Rio), Rio de Janeiro, Brazil, associated to* [2]
[63] *University of Chinese Academy of Sciences, Beijing, China, associated to* [3]
[64] *School of Physics and Technology, Wuhan University, Wuhan, China, associated to* [3]
[65] *Institute of Particle Physics, Central China Normal University, Wuhan, Hubei, China, associated to* [3]
[66] *Departamento de Fisica , Universidad Nacional de Colombia, Bogota, Colombia, associated to* [8]
[67] *Institut für Physik, Universität Rostock, Rostock, Germany, associated to* [12]
[68] *National Research Centre Kurchatov Institute, Moscow, Russia, associated to* [32]
[69] *Instituto de Fisica Corpuscular (IFIC), Universitat de Valencia-CSIC, Valencia, Spain, associated to* [38]
[70] *Van Swinderen Institute, University of Groningen, Groningen, The Netherlands, associated to* [43]

[a] *Universidade Federal do Triângulo Mineiro (UFTM), Uberaba-MG, Brazil*
[b] *Laboratoire Leprince-Ringuet, Palaiseau, France*
[c] *P.N. Lebedev Physical Institute, Russian Academy of Science (LPI RAS), Moscow, Russia*
[d] *Università di Bari, Bari, Italy*
[e] *Università di Bologna, Bologna, Italy*
[f] *Università di Cagliari, Cagliari, Italy*

[g] *Università di Ferrara, Ferrara, Italy*
[h] *Università di Genova, Genova, Italy*
[i] *Università di Milano Bicocca, Milano, Italy*
[j] *Università di Roma Tor Vergata, Roma, Italy*
[k] *Università di Roma La Sapienza, Roma, Italy*
[l] *AGH - University of Science and Technology, Faculty of Computer Science, Electronics and Telecommunications, Kraków, Poland*
[m] *LIFAELS, La Salle, Universitat Ramon Llull, Barcelona, Spain*
[n] *Hanoi University of Science, Hanoi, Viet Nam*
[o] *Università di Padova, Padova, Italy*
[p] *Università di Pisa, Pisa, Italy*
[q] *Università degli Studi di Milano, Milano, Italy*
[r] *Università di Urbino, Urbino, Italy*
[s] *Università della Basilicata, Potenza, Italy*
[t] *Scuola Normale Superiore, Pisa, Italy*
[u] *Università di Modena e Reggio Emilia, Modena, Italy*
[v] *Iligan Institute of Technology (IIT), Iligan, Philippines*
[w] *Novosibirsk State University, Novosibirsk, Russia*

[†] *Deceased*